CHAPTER 6

$M(PH_3)_2$ EXOHEDRAL METALLOFULLERENES

Since organometallic complexes of fullerenes were first prepared, many transition metals exohedral to the fullerene cages have been synthesized and structurally characterized. They are known as exohedral metallofullerenes. The first well-defined transition-metal derivative of C_{60}, $C_{60}(t\text{-}BuC_5H_5N)_2OsO_4$, was reported by Hawkins in 1991. Subsequently, a variety of exohedral metallofullerenes were synthesized because they are easy to make, isolate and characterize. Theoreticians have made numerous calculations to fit the geometry, and explain the isomerism and the addition patterns. So, unlike the two previous metallofullerenes, these fullerenes have already been studied by many researchers. We shall do our best not to be repetitive. We focus on making reliable calculations with basis set superposition error (BSSE) corrections for $M(PH_3)_2$ (M = Pt, Pd, Ni) units added to C_{60}, C_{70} and higher fullerenes such as C_{84} isomers. We also discuss aspects that have not been fully solved before such as (1) the pyramidalization effect on the strength of the fullerene-metal bond and (2) the prediction of the most reactive site of each fullerene from the characteristics of the C–C bonds.

After an introduction to previous experimental and theoretical work (section 6.1), the nature of the fullerene-metal interactions is explored through the Dewar-Chatt-Duncanson model (section 6.2). In section 6.3 we perform calculations with a large basis set to obtain reliable fullerene-metal binding energies (BE). We use additional calculations with several alternative strategies to reduce the computational effort when much higher systems

*need to be calculated. The basis sets need not be of such good quality to fit the geometry well, although they must be relatively large if the BE are to be reliable. Section 6.4 studies the addition of multiple metal units $M(PH_3)_2$ (M = Pt, Pd, Ni) to the C_{60} surface. The pyramidalization angle (θ_p) of carbons is introduced as a valuable parameter for determining the stability of the final complexes. Complementary calculations are performed on C_{70}, D_{2d}-C_{84}:**23** and D_2-C_{84}:**22** fullerenes in order to determine the relationship between curvature, C–C bond type and the strength of the fullerene-metal bond (section 6.5). The BE between the $Pt(PH_3)_2$ unit and the fullerene is almost independent of the cage size and the number of metals coordinated to the fullerene surface. Contrarily, the curvature and C–C bond type are fundamental for the strength of the coordination bond. Finally, we analyze the correlation between the characteristics of the reactive C–C bonds and the strength of the future fullerene-metal (section 6.6). The C–C bonds are characterized by the Mayer bond orders (MBO), the bond lengths and their pyramidalization angles.*

6.1 INTRODUCTION

6.1.1 Experimental part

Organometallic derivatives of fullerenes have been synthesized and structurally characterized since the beginning of fullerene coordination chemistry.[1] Reviews of all the work on the reactivity of fullerenes toward transition metal compounds have already been published.[2] The addition of the $M(PR_3)_2$ (M = Pt, Pd, Ni; R = Et, Ph) units to the most common fullerene, C_{60}, was reported before the additions to other fullerenes.[3,4] With an excess of $M(PEt_3)_4$ the hexaaddition product $(\eta^2\text{-}C_{60})\{M(PEt_3)_2\}_6$ (M = Pt, Pd) was obtained.[5] Monoaddition Vaska-type complexes was also synthesized and characterized for C_{60}[6] and the higher fullerenes C_{70}[7] and C_{84}.[8] Multiple additions are also possible but they often lead to a mixture of products. Nevertheless, some double addition products of C_{60} and C_{70} were well determined: $(\eta^2\text{-}C_{60})\{Ir(CO)Cl(PMe_2Ph)_2\}_2$,[9] $(\eta^2\text{-}C_{60})\{Ir(CO)Cl(PR_3)_2\}_2$ (R = Et, Me)[10] and $(\eta^2\text{-}C_{70})\{Ir(CO)Cl(PMe_2Ph)_2\}_2$.[11] In conclusion, most synthesized exohedral metallofullerenes are based on electron-rich transition metals, such as those in group VIII. In particular, several $(\eta^2\text{-}C_{60})M(PR_3)_2$ complexes of the Ni, Pd and Pt triad with R = Et, Ph were synthesized and the Pd and Pt complexes were structurally characterized. It is important to notice that the reactions which lead to these exohedral complexes are reversible, so, the thermodynamic product is always found.

These exohedral metallofullerenes are synthesized in solution and one of their notable features is the ease with which many of them can be made, and the ready isolation of crystalline derivatives, which can be examined by X-ray crystallography. This technique has been of great value in determining both the structures of the fullerene cages and the location of the metal units. NMR spectroscopic observations that focus for example, on ^{31}P spectra of metals bound to phosphines or ^{13}C spectra of fullerenes have also proven to be useful structural techniques. UV/vis absorption spectra and infrared spectroscopy are also spectroscopic techniques that can be used for characterization.

Although all the carbons in C_{60} are chemically equivalent, two different C–C bond types can be distinguished for the 6:6 and 6:5 ring

junctions: pyracylene and corannulene C–C bond types, respectively (***A*** and ***D*** types in Appendix A.2, respectively). So far, metals have only been attached to electron-rich pyracylene 6:6 C–C bond types. For the multiple metal additions, an extended Hückel analysis of the (η^2-C$_{60}$)Pt(PH$_3$)$_2$ complex revealed a slight preference for the second addition to occur at the opposite 6:6 C–C bond. It was also experimentally corroborated for the double addition of iridium compounds.[12] The hexaaddition derivatives of platinum and palladium have almost T_h symmetry, each one of the metals being bound to a 6:6 C–C bond, as in the (η^2-C$_{60}$){Pt(PPh$_3$)$_2$}$_6$ complex. Only one isomer obeys the isolated pentagon rule (IPR) for the C$_{70}$.[13] This structure, which has a D_{5h} symmetry, has five types of carbons that form nine layers. Eight types of C–C bonds connect these carbons, four of which occur at 6:6 ring junctions: Ca–Cb, Cc–Cc, Ce–Ce and Cd–Ce (Figure 6.1 and Appendix A.4). The first two C–C bonds are pyracylene types while the third is a pyrene type (***A*** and ***C*** types in Appendix A.1). In the (η^2-C$_{70}$)Ir(CO)Cl(PPh$_3$)$_2$ Vaska-type complex the Ca–Cb position is preferred. The reaction of C$_{70}$ with an excess of Ir(CO)Cl(PMe$_2$Ph)$_2$ produced exclusively the (η^2-C$_{70}$)Ir(CO)Cl(PMe$_2$Ph)$_2$, a double addition in two Ca–Cb bonds. Also, the reaction of C$_{70}$ with the (η^2-C$_2$H$_4$)Pt(PPh$_3$)$_2$ led to the four adducts: the (η^2-C$_{70}$){Pt(PPh$_3$)$_2$}$_n$ where n = 1-4. For the tetraaddition complex, the first two additions take place at the Ca–Cb bonds, at opposite ends of the fullerene, whereas the next two additions occur at the Cc–Cc bonds, also on opposite sides of the cage.[14] The structure of the C$_{84}$ fullerene is more complex because it has 24 IPR isomers. It shall therefore be discussed in detail below. Theoretical calculations indicate that isomers **22** and **23** of symmetries D_2 and D_{2d}, respectively, have the lowest energies.[15] Both isomers can be converted into each other through the Stone-Wales transformation.[16] ^{13}C NMR studies on C$_{84}$ confirm the presence of two isomers in a 2:1 mixture favorable to the D_2-C$_{84}$:**22** isomer.[17] However, the X-ray diffraction of the (η^2-C$_{84}$)Ir(CO)Cl(PPh$_3$)$_2$ complex, synthesized from the addition of an excess of Ir(CO)Cl(PPh$_3$)$_2$ to a mixture of C$_{84}$ isomers, showed that the prevalent geometry of the fullerene portion corresponds to the D_{2d}-C$_{84}$:**23** structure, but that the residual presence of organometallic complexes from the other isomer can not be avoided. The D_{2d}-C$_{84}$:**23** isomer has 19 different sets of C–C bonds (Figure

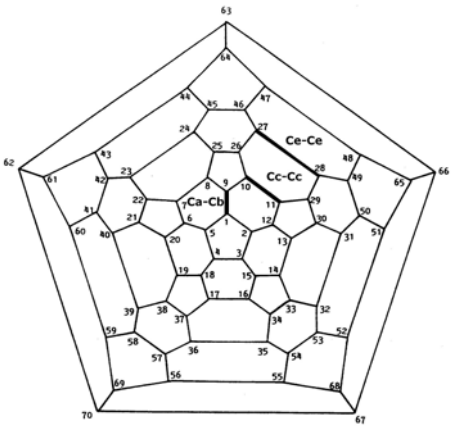

(a) Schlegel diagram of D_{5h}-C_{70}:**1**

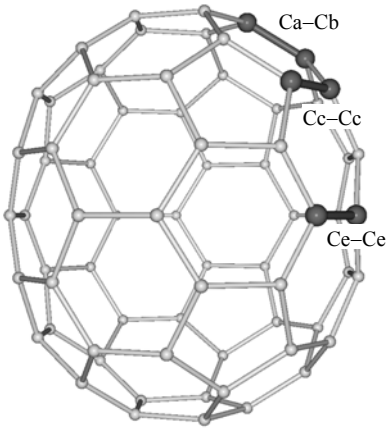

(b) Structure of D_{5h}-C_{70}:**1**

Figure 6.1 Schlegel diagram (a) and molecular structure (b) of the D_{5h}-C_{70}:**1** that incorporate the different set of C–C bonds studied. The D_{5h}-C_{70} molecule is formed by five different carbons situated in nine layers, and eight distinct set of C–C bonds. Of the four 6:6 C–C bond types, Ca–Cb, Cc–Cc, Ce–Ce and Cd–Ce, only two are of pyracylene types (***A*** type), Ca–Cb and Cc–Cc. Ce–Ce is of pyrene type (***C*** type) and Cd–Ce is of ***B*** type (See Appendix A.4). The bold lines show the C–C bonds where the $Pt(PH_3)_2$ units are added. Ca–Cb in (b) is the C1–C9 in (a). Cc–Cc in (b) is the C10–C11 in (a). Ce–Ce in (b) is the C27–C28 in (a).

6.2 and Appendix A.8) whereas the D_2-C_{84}:**22** isomer shows more variability: 32 different sets of C–C bonds (Figure 6.3 and Appendix A.7). According to the X-ray diffraction, Ir atoms are coordinated to C32–C53 bond —a pyracylene type— in the Vaska-type complex abovementioned. Note, that all metal additions in the three free fullerenes take place at pyracylene 6:6 C–C bond types.

6.1.2 Theoretical part

Earlier quantum chemistry calculations at the Hartree-Fock level on $(\eta^2$-$C_{60})\{M(PH_3)_2\}_n$ (M = Pd, Pt; n = 1, 2, 6) complexes showed that the hemisphere of the C_{60} cage which is furthest from the platinum coordination is essentially unperturbed by the metal addition.[18,19] The computed

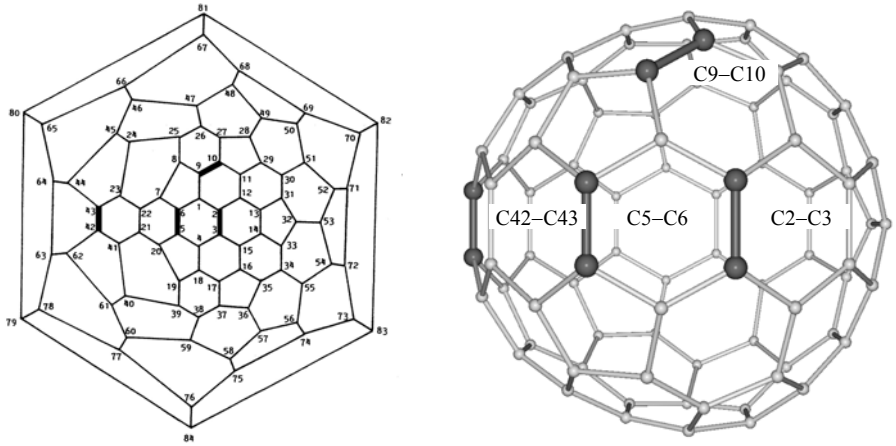

(a) Schlegel diagram of D_{2d}-C_{84}:**23** (b) Structure of D_{2d}-C_{84}:**23**

Figure 6.2 Schlegel diagram (a) and molecular structure (b) of the D_{2d}-C_{84}:**23** isomer that incorporate the different set of C–C bonds studied. We used the same atom numbering outlined in reference 40. Both drawings have the same orientation to facilitate comparison. The bold lines show the C–C bonds which have Pt(PH$_3$)$_2$ units attached.

geometries for these complexes at the HF level are in reasonably good agreement with experimental X-ray data but the calculated binding energies (BE) between the metal and fullerene cages are unreliable at that computational level because the electronic correlation effects are considerable. More recently, Sgamellotti made a detailed analysis of the fullerene-metal bond in the (η^2-C_{60})M(PH$_3$)$_2$ complexes for M = Ni, Pd, Pt.[20,21] Since complex formation causes only a local structural deformation of the fullerene cage, the pyracylene model was proposed for substituting C_{60} in the fullerene-metal interaction. To our knowledge, no quantum chemistry calculations of the organometallic derivatives of higher fullerenes have been reported yet. Dedieu made an in-depth discussion about the DE of the ethylene complexes of Pd and Pt such as (η^2-C_2H_4)M(PR$_3$)$_2$ (M = Pd, Pt).[22] These complexes are experimentally well-known and appear very often as key intermediates in a variety of reactions that are mediated or catalyzed by transition metals.

Litchtenberger systematically examined the bond between a palladium atom or a silver (I) ion and C_{60} at five different sites on the

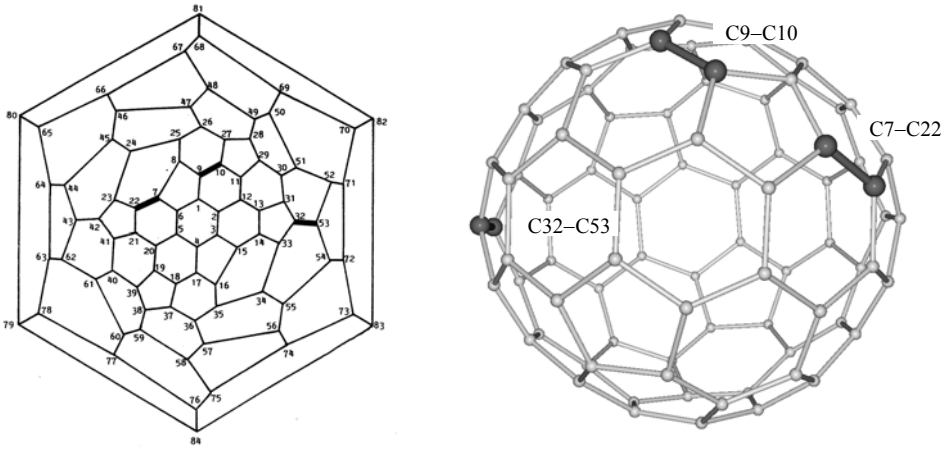

(a) Schlegel diagram of D_2-C_{84}:**22** (b) Structure of D_2-C_{84}:**22**

Figure 6.3 Schlegel diagram (a) and molecular structure (b) of the D_2-C_{84}:**22** isomer that incorporate the different set of C–C bonds studied. We used the same atom numbering outlined in reference 40. Both drawings have the same orientation to facilitate comparison. However, both drawings represent two distinct enantiòmers. This is possible because the D_2-C_{84}:**22** isomer is a chiral molecule. So both drawings are connected symmetrically by a mirror plane. The bold lines show the C–C bonds which have $Pt(PH_3)_2$ units attached.

fullerene surface. He concluded that only η^2 and η^5 coordination are favored but the former is always preferred to the latter.[23] Even so, the transition-metal fragment in most organometallic complexes is bound to the fullerene in a η^2 coordination. Recently calculations carried out at the semiempirical PM3 level on a series of $C_{60}M(C_nH_n)$ and $C_{70}M(C_nH_n)$ complexes have suggested that it is possible to stabilize η^6 coordination complexes of C_{60} and C_{70} using appropriate transition-metal fragments.[24] The interaction between a transition-metal complex and a π system in a η^2 coordination is generally described by the Dewar-Chatt-Duncanson model.[25]

The structures for these addition products suggest that a high fullerene curvature significantly enhances the reactivity of the fullerene, and facilitates the addition of the functional groups. Accordingly, in C_{70}, the metal atom is added to the most pyramidalised carbons and in the organometallic complex the pyramidalization of these atoms increases significantly.[26] The relationship between the local atomic structure and the

chemical reactivity of fullerenes was characterized by Haddon using the pyramidalization angle (θ_p) of carbons.[27] The regiochemistry will be dominated not only by the pyramidalization angles but also by the bond orders and bond lengths. Without doubt a positive correlation between π-bond order and the BE for the complexes is expected.

6.2 COORDINATION BOND BETWEEN THE FULLERENE CAGE AND THE METAL UNIT

6.2.1 Structure of (η^2-C$_{60}$)Pt(PH$_3$)$_2$

The first calculations dealt with (η^2-C$_{60}$)Pt(PH$_3$)$_2$ as a model of the η^2 coordination of the Pt(PPh$_3$)$_2$ unit to the C$_{60}$ fullerene: (η^2-C$_{60}$)Pt(PPh$_3$)$_2$. Ph groups are modelled by hydrogen atoms. This structure was the first transition-metal complex to have direct bonds to C$_{60}$ and also the first of this family of complexes to be determined by X-ray diffraction. So, a full understanding of the metal bond established in the (η^2-C$_{60}$)Pt(PH$_3$)$_2$ complex can be representative of the metal bond in the exohedral metallofullerenes studied in this chapter. The fullerene-metal bond in these transition-metal complexes can also be also easily understood by comparing the bonding characteristics in the analogous complexes of ethylene and tetracyanoethylene (TCNE): (η^2-C$_2$H$_4$)Pt(PH$_3$)$_2$ and (η^2-C$_2$(CN)$_4$)Pt(PH$_3$)$_2$. In all the transition-metal fullerene complexes characterised, fullerenes act as electron-deficient polyalkenes because their physical and chemical properties have similar values to those found for polyalkenes such as TCNE. For instance, the experimental electron affinity of C$_{60}$, 2.7 eV,[28] is very close to that of TCNE, the experimental and theoretical values of which are 2.88 eV[29] and 3.51 eV, respectively. Table 6.1 lists the calculated electron affinities (EAs) and ionization potentials (IPs) of the three ligands. According to the calculated values of the EAs, C$_{60}$ and TCNE have electron attracting character —positive values— whereas C$_2$H$_4$ has a negative value of the EA, which indicates non electron attracting character. In consequence, only C$_{60}$ and TCNE are expected to accept electrons easily. The similarity between the C$_{60}$ and TCNE complexes can also be seen in geometrical aspects: the Pt–C bond length in the (η^2-C$_{60}$)Pt(PH$_3$)$_2$ complex (2.139 Å) is closer to that of the corresponding (η^2-C$_2$(CN)$_4$)Pt(PH$_3$)$_2$

complex (2.136 Å) than to that of the ethylene complex (2.148 Å). This similarity also appears in the coordinated C–C bond lengths and the Pt–P bond lengths. It is therefore worth comparing the electronic structure of the fullerene complexes with that of the ethylene and TCNE complexes. The special stabilization when the metal unit is attached to the fullerene is corroborated by the high HOMO-LUMO gaps for these complexes: 1.38 eV for (η^2-C_{60})Pt(PH_3)$_2$, 4.00 eV for (η^2-C_2H_4)Pt(PH_3)$_2$ and 3.37 eV for (η^2-$C_2(CN)_4$)Pt(PH_3)$_2$. It shall also be interesting to compare this series of model complexes with the previously calculated platinum complex: (η^2-C_2H_4)C_{58}Pt (named C_{58}Pt(C_2H_4) in Chapter 5).[30] This is a monoheterofullerene with an ethylene coordinated to the Pt atom and, unlike the exohedral metallofullerenes shown in this chapter, the Pt atom takes part of the fullerene unit and not part of the ligand.

Some brief comments should be made about the different possible conformers of these M(PH_3)$_2$ exohedral metallofullerenes. The most important feature of these exohedral complexes is that the metal diphosphines are η^2 coordinated to a 6:6 C–C bond. All the X-ray structures available for metal diphosphine fullerene complexes align the 6:6 C–C edge in the MP_2 plane rather than perpendicular to it, just as the corresponding ethylene complexes do. All geometry optimizations on the fullerene complexes were therefore performed in the parallel orientation with imposed C_{2v} symmetry constraints. It is important to point out that the most stable conformer is that in which the hydrogens in the metal unit are eclipsed; other conformers have only slightly different relative energies.

The optimised geometries of these first three complexes are collated in Table 6.1. Metal addition causes a similar distortion in all the complexes: (1) a lengthening of the C–C bond lengths from the free ligand to the complex by about 0.086-0.127 Å and (2) a pulling away the C–C edge from the fullerene surface, which is shown in the increase in the pyramidalization angle of the coordinated carbons from the free ligand to the complex: 8.42°, 6.66° and 3.69° for ethylene, TCNE and fullerene complexes, respectively. Notice that the carbons of free ethylene and TCNE are not pyramidalized. The addition reaction is accompanied by the formation of σ and π Pt–C bonds and a partial breaking of the π bond of the C=C bond of the fullerene. This indicates that the coordinated carbons will increase their sp^3 character in the complex. The Pt–C bond lengths were determined to be 2.139 Å,

Table 6.1 Description of A-B interactions, A is a ligand and B is a molecule containing a metal atom. A-B is a stable complex [a]

A-B		(η^2-C_2H_4)-$C_{58}Pt$	(η^2-C_2H_4)-$Pt(PH_3)_2$	(η^2-$C_2(CN)_4$)-$Pt(PH_3)_2$	(η^2-C_{60})-$Pt(PH_3)_2$
A-B	Pt (in B)–C (in A)	2.447	2.148	2.136	2.139
	Pt (in B)–P (in B)	--	2.294	2.297	2.297
	C–C	1.373	1.432	1.507	1.495
	θ_p [b]	2.89	8.42	6.66	15.36
	P–Pt–P ang.	--	106.4	99.9	106.3
	Elect transf. B $\rightarrow$ A	–0.166	0.316	0.846	0.688
A	θ_p	0.00	0.00	0.00	11.67
	C–C	1.334	1.334	1.380	1.397
	MBO [c]	1.821	1.821	1.486	1.342
	Electron affinity [d]	–1.82 (–1.6) [f]	–1.82 (–1.6) [f]	3.51 (3.2) [g]	2.89 (2.7) [h]
	Ionization potential [d]	10.51 (10.5) [i]	10.51 (10.5) [i]	11.12 (11.8) [j]	7.56 (7.6) [k]
BE [e]		–0.70	–0.89	–1.39	–0.96

[a] Distances in Å, angles in º and energies in eV. [b] The carbons of the free alkene are not pyramidalised (θ_p = 0.00°) but the carbons of the free C_{60} have a θ_p = 11.67°. [c] Mayer bond order (MBO). [d] The experimental values are shown in parenthesis. [e] The binding energy (BE) is the energy difference between the optimized A–B adduct and the two relaxed A and B fragments. [f] Burrow, P. D.; Jordan, K. D. *Chem. Phys. Lett.* **1975**, *36*, 594. [g] Chowdhury, S.; Kebarle, P. *J. Am. Chem. Soc.* 1986, *108*, 5453. [h] Yang, S. H.; Pettiette, C. L.; Concienciao, J.; Cheshnowsky, O.; Smalley, R.E. *Chem. Phys. Lett.* **1991**, *139*, 233. [i] Lias, S. G.; Bartmess, J. E., Liebman, J. F.; Holmes, J. L.; Levin, R. D.; Mallard, W. G. Gas-Phase Ion and Neutral Termochemistry, *J. Phys. Chem.* Ref. Data Vol. 17, Suppl. No. 1, **1998**. [j] Stafast, H.; Bock, H. *Tetrahedron* **1976**, *32*, 855. [k] Lichtenberger, D. L.; Nebesny, K. W.; Ray, C. D.; Huffman, D. R.; Lamb, L. D. *Chem. Phys. Lett.* **1991**, 176, 203.

2.136 Å and 2.148 Å for (η^2-C_{60})$Pt(PH_3)_2$, (η^2-$C_2(CN)_4$)$Pt(PH_3)_2$ and (η^2-C_2H_4)$Pt(PH_3)_2$, respectively, and are a measure of the strength of the ligand-metal bond. From the structural information available, one can conclude that coordination in C_{60} and TCNE will be stronger than in ethylene. On the

other hand, the Pt–C bond lengths in the (η^2-C_2H_4)C_{58}Pt complex were computed to be much longer (2.447 Å) which indicated that the metal bond is weaker than the other types of fullerene-metal complexes. Specifically, in the most important model molecule, the (η^2-C_{60})Pt(PH_3)$_2$, the results of the geometry optimization of the complex give an evidence of a local structural deformation of the C_{60} unit, mainly localized in the interaction region. The C–C bond directly bound to the metal fragment increases in length by 0.098 Å and the pyramidalization angle increases from 11.67° in the free fullerene to 15.47° in the complex. Despite this, the opposite side of the fullerene remains almost unperturbed. The P–Pt–P angle reduces from its free value of 180° up to 106.3° in the complex and this change and the modification in the Pt–P bond lengths can be taken as a measure of the distortion of the Pt(PH_3)$_2$ unit.

6.2.2 The Dewar-Chatt-Duncanson model

The most widely accepted model for the patterns of (η^2-C_{60})M bonds is that proposed by Dewar, Chatt and Ducanson. It involves forming a σ-donation bond from the π C–C orbitals of the ligand to the metal and a π-back-donation bond from the metal *d*-orbitals to the π* C–C orbitals of the ligand. Thus, the π C–C bond of the ligand is weakened by the σ-donation which means that the energy of the π* C–C orbital decreases, so it can easily accept electrons from a back-donating *d*-orbital of the metal. The π interaction should be dominant for a d^{10} metal, and show a certain tendency to electron charge transfer from the metal to the C–C bond. On the other hand, the key point to bear in mind is the remarkable tendency of fullerenes to accept electrons. The combination of both effects leads to two different cases: (1) a considerable electron charge transfer from the *d* metal orbitals to the fullerene ligand for (η^2-C_{60})Pt(PH_3)$_2$ (0.688 *e*), for (η^2-$C_2(CN)_4$)Pt(PH_3)$_2$ (0.846 *e*) and for (η^2-C_2H_4)Pt(PH_3)$_2$ complex (a lower value of 0.316 *e*); and (2) an electron charge transfer from the ethylene ligand to the *d* metal orbital of the (η^2-C_2H_4)C_{58}Pt monoheterofullerene (0.086 *e*) (Table 6.1). These values are calculated from the Mulliken net charges. The amount of electron charge transfer in C_{60}-metal and TCNE-metal complexes is about twice that

in the ethylene-metal complex. This gives us complementary ideas about the strength of the ligand-metal bonds.

The BE is the energy difference between the optimized A–B complex and the two relaxed A and B fragments. The DE is defined as –BE. The order of the BE for the complexes is: (η^2-C$_2$(CN)$_4$)Pt(PH$_3$)$_2$ > (η^2-C$_{60}$)Pt(PH$_3$)$_2$ > (η^2-C$_2$H$_4$)Pt(PH$_3$)$_2$ > (η^2-C$_2$H$_4$)C$_{58}$Pt. The BE for the fullerene-metal was calculated as –0.96 eV and found to be higher than the corresponding ethylene-metal, –0.89 eV, but lower than the TCNE-metal, –1.39 eV. To separate the contributions from the σ donation and π back-donation, we analysed the ligand-metal bond DEs by using the extended transition method developed by Ziegler and Rouk,[31] which is an extension of the Morokuma's well-known decomposition.[32] The DE can be decomposed into several contributions: ΔE_{DE}, ΔE_{ST}, ΔE_{ORB}. More details about this decomposition can be found in subsection 4.2.4. ΔE_{ORB} term may be broken up into contributions from the orbital interactions within the various irreducible representations of the overall symmetry group of the system, according to the decomposition scheme proposed by Ziegler. The σ donation takes places in the a_1 representation whereas the π back-donation takes place in the b_1 representation. The decomposition for all model complexes is shown in Table 6.2.

A detailed comparison of the decomposition of the BE confirms that the coordinated bond between C$_{60}$ and the Pt(PH$_3$)$_2$ unit is qualitatively more similar to electron-deficient alkene complexes such as TCNE than ethylene. The BE for (η^2-C$_2$(CN)$_4$)Pt(PH$_3$)$_2$ is 0.50 eV higher than for (η^2-C$_2$H$_4$)Pt(PH$_3$)$_2$ and 0.43 eV higher than for (η^2-C$_{60}$)Pt(PH$_3$)$_2$. The term responsible for these energy differences is ΔE_{ORB}. Specifically, these are due to the π back-donation since σ donation remains almost constant (*ca.* 1.4-1.5 eV) for all complexes. The π back-donation in the C$_{60}$ and TCNE complexes is much larger than in the ethylene complex. It is clear that the contribution to the ΔE_{ORB} term from the π back-donation dominates over that from the σ donation in this kind of exohedral metallofullerenes. The π back-donation changes from –2.68 eV for (η^2-C$_2$H$_4$)Pt(PH$_3$)$_2$ to –4.69 eV for (η^2-C$_2$(CN)$_4$)Pt(PH$_3$)$_2$. Finally, note that the highest destabilization of ΔE_{DE} and ΔE_{ST} values for (η^2-C$_2$(CN)$_4$)Pt(PH$_3$)$_2$ are not enough to neutralize the high stabilization produced by the π back-donation and consequently it has the

Table 6.2 Decomposition of the binding energy (BE) for series that represents A-B interactions [a]

A-B		*(η^2-C_2H_4)-$C_{58}Pt$* [b]	*(η^2-C_2H_4)-$Pt(PH_3)_2$*	*(η^2-$C_2(CN)_4$)-$Pt(PH_3)_2$*	*(η^2-C_{60})-$Pt(PH_3)_2$*
ΔE_{DE}	*Metal unit*	0.14	0.54	1.34	0.38
	Lligand	0.07	1.11	0.75	1.14
	Total	0.21	1.65	2.09	1.52
ΔE_{ST}	ΔE_{Pauli}	4.72	9.00	9.31	9.17
	ΔE_{elstat}	–3.20	–7.11	–6.34	–6.55
	Total	1.52	1.89	2.97	2.62
ΔE_{ORB}	$\Delta E_{a1}(\sigma)$	–1.58	–1.53	–1.34	–1.39
	ΔE_{a2}	–0.03	–0.02	–0.08	–0.04
	$\Delta E_{b1}(\pi)$	–0.73	–2.68	–4.69	–3.41
	ΔE_{b2}	–0.09	–0.20	–0.34	–0.26
	Total	–2.43	–4.43	–6.45	–5.10
ΔE_{INT}		–0.91	–2.53	–3.48	–2.48
BE [c]		–0.70	–0.89	–1.39	–0.96

[a] Values in eV. [b] In Chapter 5 is named $C_{58}Pt(C_2H_4)$ (see ref. 30). [c] The binding energy (BE) is the energy difference between the optimized A–B adduct and the two relaxed A and B fragments.

highest BE of the complexes studied. That the BE is stronger for C_{60} than ethylene is in line with Morokuma and Borden's previous findings,[33] that the strain (in C_{60}) decreases the π^* orbital energy and increases π back-donation.

The different reactivity of the series: (η^2-C_2H_4)$Pt(PH_3)_2$, (η^2-C_{60})$Pt(PH_3)_2$ and (η^2-$C_2(CN)_4$)$Pt(PH_3)_2$ can be predicted using the Mayer bond order (MBO) of the free C–C bonds. A strong C–C bond with a high π-bond order should increase the σ donation and the π back-donation, and consequently, the BE between both fragments. This argument is completely reliable for ligands with similar electron affinities such as fullerenes and electron deficient alkenes (*e.g.* TCNE) but not for ethylene. The MBO for

the 6:6 C–C bond of C_{60} is computed to be 1.342 and for ethylene 1.821, but even so, the BE for the latter is much lower than for the former by 0.07 eV. This can be explained by taking into account that C_{60} and $C_2(CN)_4$ have a more attracting electron character (higher EA) than ethylene, while the ionization potentials are similar (Table 6.1).

Now let us turn our attention to the (η^2-C_2H_4)C_{58}Pt complex. The geometrical coordination of the various complexes led us to expect that it would be the least stable. Indeed, –0.70 eV of BE compared to –0.96 eV for the fullerene-metal bond. The consequence is a longer Pt–C distance and no elongation of ethylene C–C bond lengths. This can be attributed to the almost non-existent π back-donation from the metal atom to the ethylene in this complex. Although the σ donation is the same as that of the other Pt complexes (≈ 1.5 eV) and even the ΔE_{ST} and ΔE_{DE} terms are more favorable to the (η^2-C_2H_4)C_{58}Pt formation than in the other complexes, all these terms are not enough to counteract the lack of π back-donation. This weak π back-donation can be explained from two points of view: (1) there are no *d* metal orbitals available to connect to π* C–C of the ligand because they are involved in the bond of the fullerene carbon framework (Chapter 5); (2) the electron donor character of the such monoheterofullerenes as free fullerenes is weak. The EA of the C_{58}Pt, 3.67 eV, is even higher than that of C_{60}, so the π back-donation from C_{58}Pt to ethylene is not favoured at all, unlike the (η^2-C_{60})Pt$(PH_3)_2$ complex where the π back-donation represents the electron charge transfer from the Pt$(PH_3)_2$ unit to the C_{60} fullerene. So, for all the Pt complexes studied, except (η^2-C_2H_4)C_{58}Pt, the bonding contribution from the π back-donation dominates over that from the σ donation.

6.3 MONOADDITION COMPLEXES OF C_{60} AND ETHYLENE

6.3.1 Pt complexes

The addition of a Pt$(PH_3)_2$ unit to C_{60} in a 6:6 C–C bond generate a certain distortion in the fullerene cage, mainly in the interacting region (Figure 6.4). As a result, the coordinated C–C bond increased to 1.495 Å in the complex. This computed distance only slightly differs with the X-ray

value reported for (η^2-C_{60})Pt(PPh_3)$_2$, 1.502 Å. The deviations of the computed Pt–P and Pt–C bond lengths from the experimental values were found also very small as Table 6.3 shows.

The DE of (η^2-C_{60})Pt(PH_3)$_2$ to give the fullerene and the metal unit was computed to be 0.96 eV, a relatively high energy that stresses the stability of the organometallic derivatives of C_{60}. The hypothetical isomer with the metal linked to a 6:5 C–C bond was also studied. This isomer is 0.51 eV less stable than the observed cluster with the metal atom bonded to a 6:6 C–C bond. In agreement with the lower cage-metal interaction in the 6:5 complex, the Pt–C bond distance in this isomer is 0.042 Å longer than in the 6:6 complex and the P–Pt–P angle is somewhat greater: 112.5º and 106.3º in the 6:5 and 6:6 complexes, respectively.

The (η^2-C_{60})Pt(PR_3)$_2$ monoaddition complex is prepared through the substitution reaction:

(6.1) $$(\eta^2\text{-}C_2H_4)Pt(PR_3)_2 + C_{60} \rightarrow (\eta^2\text{-}C_{60})Pt(PR_3)_2 + C_2H_4$$

Reaction 6.1 is exothermic by only 0.07 eV with a triple-ζ + polarization (TZP) Slater basis set for all atoms. So, whereas the DE for the fullerene complex is 0.96 eV, the corresponding value for the ethylene precursor is 0.89 eV. This difference seems very small and in fact the DE of the ethylene-metal has been reported to be 0.99 eV at NL-DFT+QR level[34] and 1.22 eV at the CCSD(T) level.[35] It still remains some discrepancy with the experimental calorimetric studies for (η^2-C_2H_4)Pt(PPh_3)$_2$ which leads to an estimation of 1.56 ± 0.17 eV for the DE of C_2H_4–Pt.[36] Rosa et al. have shown that the basis set superposition errors (BSSE) are very small when these relatively large basis sets are used. In transition-metal complexes the BSSE has been estimated to be typically between 0.04-0.08 eV with TZP basis set[37] and therefore this correction at this level of computation can be neglected. The calculated BSSE was also found in this order of magnitude for our complexes using TZP Slater basis set: 0.05 eV for (η^2-C_{60})Pt(PH_3)$_2$ and 0.02 eV for (η^2-C_2H_4)Pt(PH_3)$_2$. All geometries and BE for the above mentioned exohedral metallofullerenes with different basis set are collated in Table 6.3. Notice that all BE do not include BSSE corrections but this term is listed near the BE values.

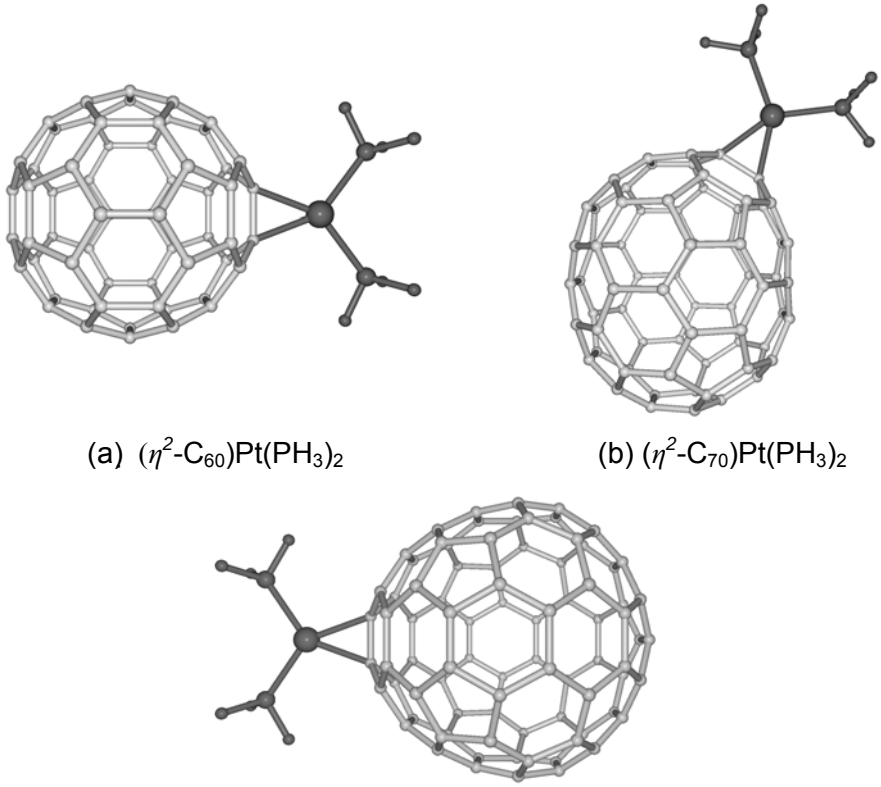

Figure 6.4 The structure of the most stable isomers of (η^2-C$_{60}$)Pt(PH$_3$)$_2$, metal unit linked to the 6:6 C–C bond type (a); (η^2-C$_{70}$)Pt(PH$_3$)$_2$, metal unit linked to the Ca–Cb bond (b), and (η^2-C$_{84}$)Pt(PH$_3$)$_2$, metal unit linked to the C42–C43 bond (c).

With the perspective of studying larger fullerene-metal systems than those reported herein, we analyzed the effect of the basis set on the DE and geometries. If the C$_{60}$ is described by a double-ζ + polarization (DZP) Slater basis set and the Pt moiety by a TZP the geometry hardly changes but the DE increases up to 1.41 eV, whereas the corresponding value for ethylene precursor is 0.92 eV. Furthermore, higher BSSE corrections were obtained when the DZP Slater basis set were used for the ligand (fullerene/ethylene): 0.37 eV for fullerene-metal complex and 0.10 eV for ethylene-metal

Table 6.3 DFT geometries and binding energies (BE) for the (η^2-C_{60})$Pt(PH_3)_2$ complex and for the (η^2-$C_{14}H_8$)$Pt(PH_3)_2$ and (η^2-C_2H_4)$Pt(PH_3)_2$ model complexes [a]

Molecule	*Basis set*	*Pt–P*	*Pt–C*	*C–C*	*BE* [b]	*BSSE*
(η^2-C_{60})$Pt(PPh_3)_2$ [c,f]		2.278	2.130	1.502	--	--
(η^2-C_{60})$Pt(PH_3)_2$ [e,g]	TZP	2.297	2.139	1.495	–0.96	0.05
	C(DZP); C,P,H,Pt(TZP)	2.293	2.120	1.504	–1.07	0.09
	C(DZP); P,H, Pt(TZP)	2.297	2.137	1.495	–1.41	0.37
(η^2-$C_{14}H_8$)$Pt(PH_3)_2$ [d,g]	TZP	2.271	2.065	1.528	–1.21	0.08
	C, P, H (DZP);Pt(TZP)	2.277	2.112	1.503	–0.95	0.29
(η^2-C_2H_4)$Pt(PPh_3)_2$ [c,f]		2.268	2.111	1.434	--	--
(η^2-C_2H_4)$Pt(PH_3)_2$ [e,g]	TZP	2.294	2.148	1.432	–0.89	0.02
	C, H (DZP); Pt, P, H(TZP)	2.294	2.147	1.431	–0.92	0.10

[a] Bond lengths in Å, angles in º and energies in eV. [b] The BE (binding energy) is equal to the –DE (dissociation energy). [c] ref. 3. [d] ref 21. [e] This study. [f] X-ray. [g] DFT.

complex. The discrepancy observed in the DE motivated us to check a mixed basis set for the fullerene cage. That is, the reactant pyracylene unit described by a TZP and the rest of the fullerene cage by a DZP. In these conditions, the X-ray geometry is well reproduced (Table 6.3) and the DE was now computed to be 1.07 eV, only 0.11 eV higher than that found with the large TZP Slater basis set; the BSSE correction is also quite small, 0.09 eV. It should also be pointed out that the energies of the frontier orbitals are very similar to those found with the TZP basis: with the mixed basis, the HOMO and LUMO energies are –5.97 eV and –4.64 eV; while the corresponding values with the largest basis set are –5.54 eV and –4.16 eV, respectively. This point is very important for describing the chemical properties of the complex.

An alternative process has been proposed by Sgamellotti and co-workers. They have used a pyracylene unit as model for the C_{60} cage in the (η^2-C_{60})$Pt(PH_3)_2$ to reduce the size of the system. When a DZP basis set is used for carbon, phosphorous and hydrogen and a TZP basis set is used for

Table 6.4 DFT geometries and binding energies (BE) for (η^2-C$_{60}$)M(PH$_3$)$_2$ and (η^2-C$_2$H$_4$)M(PH$_3$)$_2$ (M = Pd, Ni) [a]

Molecule	Basis set	*M–P*	*M–C*	*C–C* [b]	*BE*
(η^2-C$_{60}$)Pd(PPh$_3$)$_2$	X-ray	2.323	2.105	1.447	--
(η^2-C$_{60}$)Pd(PH$_3$)$_2$	TZP	2.348	2.175	1.467	–0.88 [d]
	C, P, H (DZP); Pt (TZP) [c]	2.378	2.180	1.464	–1.00 [e]
(η^2-C$_2$H$_4$)Pd(PH$_3$)$_2$	TZP	2.309	2.168	1.404	–0.74 [f]
(η^2-C$_{60}$)Ni(PH$_3$)$_2$	TZP	2.166	1.965	1.480	–1.73 [g]
	C, P, H (DZP); Pt (TZP) [c]	2.222	1.989	1.470	–1.70 [h]
(η^2-C$_2$H$_4$)Ni(PH$_3$)$_2$	TZP	2.146	1.987	1.410	–1.55 [i]

[a] Bond lengths in Å, angles in º and energies in eV. [b] The C–C distances in the free C_2H_4 and C_{60} are 1.334 Å and 1.397 Å, respectively. [c] From ref. 20. [d] BSSE = 0.05. [e] BSSE = 0.35. [f] BSSE = 0.02. [g] BSSE = 0.10. [h] BSSE = 0.35. [i] BSSE = 0.05.

platinum, the DE for (η^2-C$_{14}$H$_8$)Pt(PH$_3$)$_2$ is 0.95 eV but with a large BSSE of 0.29 eV, although if a TZP basis set is used to describe all atoms the DE becomes 1.21 eV and a BSSE of only 0.08 eV (Table 6.3). However, the geometry of the monoaddition complex is not properly reproduced even if this larger basis set is used: the angle P–Pt–P is always overestimated and the Pt–C bond length is predicted to be 0.065 Å shorter.

6.3.2 Pd and Ni complexes

The BE for C_{60} and ethylene complexes of Pd and Ni are tabulated in Table 6.4. The BE increases in the order Pd < Pt < Ni and fullerene complexes are always slightly more stable than ethylene complexes. The computed values are –0.88 and –1.73 for (η^2-C$_{60}$)M(PH$_3$)$_2$ complexes where M = Pd, Ni, respectively. Also the BSSE for the larger basis set was computed to be quite small, a maximum of 0.10 eV. The X-ray structure for (η^2-C$_{60}$)Pd(PPh$_3$)$_2$ is available but has not yet been reported for the nickel diphosphine complex. The geometry parameters of the (η^2-C$_{60}$)Pd(PH$_3$)$_2$

Table 6.5 Comparison of the various calculated and experimental BE of (η^2-C_2H_4)M(PH_3)$_2$ (M = Pt, Pd, Ni) ethylene complexes [a]

Method	*Pt*	*Pd*	*Ni*	*Ref.*
DFT-TZP	–0.89	–0.74	–1.55	This work
MP2 [b]	–1.07	–0.91	–1.52	19
CCSD(T) [c]	–1.22	–0.91	--	35
NL-DFT+QR [d]	–0.99	–0.86	--	34
Exp.[e]	–1.56	--	–1.30	36

[a] Values in eV. [b] Møller-Plesset. [c] Coupled cluster single, double and triple. [d] Nonlocal DFT quasirelativistic. [e] Estimated from calorimetric studies of the (η^2-C_2H_4)M(PPh_3)$_2$ complex

complex in the present results are slightly better than those reported by Sgmelloti, who used a basis set of less quality. In our calculations, the maximum deviation of the bond lengths was 0.07 Å (Table 6.4). The BE with the poorer basis set were reported by Sgmelloti to be –1.00 eV for (η^2-C_{60})Pd(PH_3)$_2$ and –1.70 eV for (η^2-C_{60})Ni(PH_3)$_2$, but if we take into account the BSSE corrections (not negligible in these cases) the values become –0.65 eV and –1.35 eV, respectively. Hence, a large basis set must be used if reliable BE are to be calculated.

On the other hand, the BE of –0.74 for the (η^2-C_2H_4)Pd(PH_3)$_2$ was underestimated in comparison with the –0.86 eV at the NL-DFT+QR level and –0.91 eV at the CCSD(T) level. Several values are reported for (η^2-C_2H_4)Ni(PH_3)$_2$ and they almost coincide with the calculated value: 1.55 eV in the present study and 1.52 eV at the MP2 level. These results are listed in Table 6.5. Unlike the (η^2-C_2H_4)Pt(PH_3)$_2$ complex, the BE for the (η^2-C_2H_4)Ni(PH_3)$_2$ matches the experimental value quite well and is only 0.25 eV bellow it. Once we calculated the BE for the ethylene and C_{60} complexes, we were able to evaluate the formation energies of the fullerene complexes from the ethylene complexes using equation 6.1 where R = H. The reaction energy is slightly exothermic in all cases following the order Pt < Pd < Ni: –0.07 eV for Pt, –0.14 eV for Pd and finally –0.17 eV for Ni.

The longest M–C distance was found in the C_{60} complex of Pd (2.175 Å) and the shortest in the C_{60} complex of Ni (1.966 Å). An intermediate distance of 2.139 Å was found for the analogous Pt complex.

These values suggest a strength of the ligand-metal bond in the following order: Pd < Pt < Ni like BE. However, this order is different if the geometrical distortion of the pyracylene patches is taken into account: Pd < Ni < Pt. This distortion is measured by the coordinated C–C bond lengths: 1.467 Å, 1.480 Å and 1.495 Å for the C_{60} complexes of Pd, Ni and Pt, respectively. Also, the cage radius increases slightly for all three complexes in the same order: Pd < Ni < Pt. Indeed, the fact that the degree of distortion of the fullerene complex of Pt is higher than that of Ni would suggest a reversed order for the strength of fullerene-metal bonds: Ni < Pt. But we have seen in the previous paragraph that the BE follows another order. This dichotomy has already been observed for olefins[38] and fullerene complexes and rationalised on the basis of the relaxation energies of the metal fragments.

6.4 POLYADDITION COMPLEXES OF C_{60}

6.4.1 Energy and geometry considerations of Pt complexes

To analyze how the multiple addition affects the BE, the series of complexes $(\eta^2\text{-}C_{60})\{Pt(PH_3)_2\}_n$ with n = 2, 4 and 6 were fully optimized. The metal units are spread further as possible to the C_{60} surface, minimizing the steric repulsion among the metal units. Several years ago, we demonstrated that the interaction is highly local and that the loss of the first platinum group in the $(\eta^2\text{-}C_{60})\{Pt(PH_3)_2\}_2$ is only slightly more favorable than the loss of the platinum group from the monoaddition derivative. The calculations that were carried out at the Hartree-Fock level, however, gave very low absolute energies (0.44 eV for the monoadduct). To check these results, we reanalyzed at the DFT level the series of complexes above mentioned with the large basis set, TZP for all atoms. Again, the optimized geometries at the present DFT level are in excellent agreement with the X-ray data available (Table 6.6). For example, for the hexaaddition complex, in which the platinum atoms are arranged in an octahedral array around the fullerene core, the computed C–C bond length is 1.487 Å while the X-ray value for $(\eta^2\text{-}C_{60})\{Pt(PEt_3)_2\}_6$ is 1.497 Å. This good agreement is also confirmed in the Pt–P and Pt–C bonds lengths where the deviations are *ca.* 0.04 Å. The deviations found at the HF level were a bit more important, *ca.*

Table 6.6 Geometric properties and fullerene-metal binding energies (BE) for (η^2-C_{60}){$Pt(PH_3)_2$}$_n$ (n = 1, 2, 4, 6) [a]

n [b]	*Sym*	*Pt–P*	*Pt–C*	*Δ(C–C)* [c]	*P–Pt–P*	*final* θ_p [d]	*BE* [e]	*BE per group* [f]
1	C_s	2.293	2.181	0.078	112.5	15.47	–0.45	–0.45
1	C_{2v}	2.297	2.139	0.098	106.3	15.36	–0.96	–0.96
2	D_{2h}	2.289	2.131	0.103	108.2	15.36	–0.80	–0.88
4	D_{2h}	2.288	2.150	0.094	107.7	15.07	–0.82	–0.85
6	T_h	2.289	2.153	0.090	108.1	14.88	–0.73	–0.81

[a] Bond lengths in Å, angles in º and energies in eV. [b] All C–C bonds are pyracylene type except the first row which is a corannulene type. [c] Difference between the original bond in the free C_{60} and in the complex. [d] Pyramidalization angle (θ_p) for the carbons attached to metal unit in the complex. The θ_p for the free C_{60} is 11.67º. [e] For n = 4 and n = 6, the binding energy (BE) is estimated from the reaction energies (η^2-C_{60}){$Pt(PH_3)_2$}$_{n-2}$ + 2{$Pt(PH_3)_2$} → (η^2-C_{60}){$Pt(PH_3)_2$}$_n$ and the tendency observed from n = 2 to n = 1. [f] The BE per group is calculated from the reaction: C_{60} + n{$Pt(PH_3)_2$} → (η^2-C_{60}){$Pt(PH_3)_2$}$_n$, BE per group = ΔE/n; ΔE, reaction energy. BSSE = 0.05-0.07 eV.

0.05 Å.[19] The Pt–C distances slightly increase as the number of metals on the fullerene surface increases. Thus, the Pt–C bond length is 2.139 Å for the monoadduct and 2.153 Å for the hexaadduct. The pyramidalization angle of the coordinated carbons to the metal augments and the maximum distortion appears in the monoaddition complex. When metals are successively added to the fullerene core the pyramidalization angle of the coordinated carbons decreases (Table 6.6 and Figure 6.5).

The present DFT calculations fully confirm that the addition of one metal group to the C_{60} only slightly reduces the ability of the carbon cluster to accept a second metal. The reaction energy for the process

(6.2) (η^2-C_{60}){$Pt(PH_3)_2$}$_2$ → (η^2-C_{60})$Pt(PH_3)_2$ + $Pt(PH_3)_2$

is found to be 0.80 eV, which is only 0.17 eV smaller than for the DE of the monoaddition complex. Thus, the BE per group is –0.88 eV for n = 2. Because of the low symmetry of the pentacoordinated complex the energy associated to the loss of the first metal group in the hexaadduct complex was not determined. Nevertheless, we calculated the reaction energy for the process

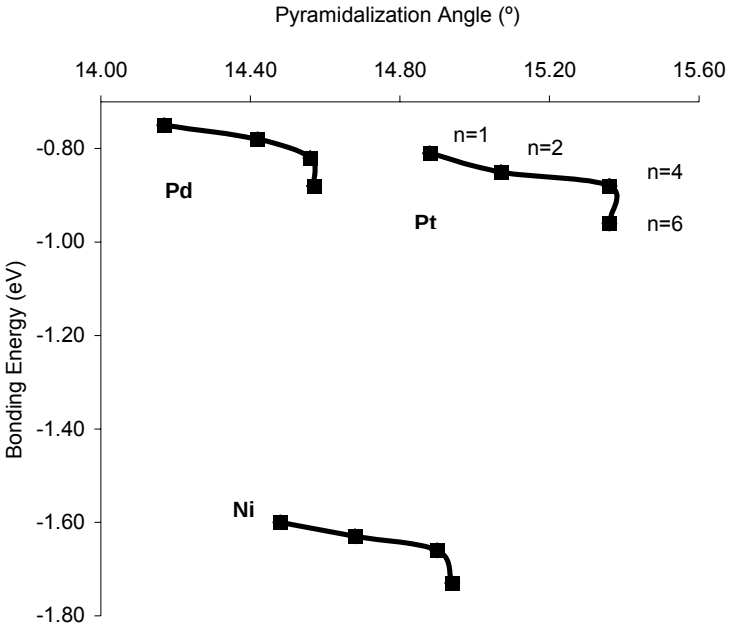

Figure 6.5 Correlation between the binding energy (BE) and the pyramidalization angle (θ_p) for (η^2-C$_{60}$){M(PH$_3$)$_2$}$_n$ (M = Pt, Pd, Ni; n = 2, 4, 6).

(6.3) $$(\eta^2\text{-C}_{60})\{\text{Pt(PH}_3)_2\}_6 \rightarrow (\eta^2\text{-C}_{60})\{\text{Pt(PH}_3)_2\}_4 + 2\{\text{Pt(PH}_3)_2\}$$

which is 1.45 eV. The tendency of the DE when going from n = 1 to n = 2 suggests that the loss of the first metal group in the (η^2-C$_{60}$){Pt(PH$_3$)$_2$}$_6$ should be almost ~ 0.64 eV ($C_{60}M_6 \rightarrow C_{60}M_5$ for short), whereas the dissociation process from $C_{60}M_5$ to $C_{60}M_4$ is estimated to be ~ 0.81 eV. The same strategy was followed for n = 4 and n = 3. The energy involved in the $C_{60}M_4 \rightarrow C_{60}M_2$ process is equal to 1.63 eV, which yields estimated values of ~ 0.73 eV and ~ 0.90 eV for $C_{60}M_4 \rightarrow C_{60}M_3$ and $C_{60}M_3 \rightarrow C_{60}M_2$, respectively. All these energies are clearly larger than the energy involved in the coordination of a platinum atom to a 6:5 ring junction, 0.45 eV. Consequently, the metal addition always takes place at the 6:6 C–C bond. To remove the six groups from the fullerene surface requires 4.84 eV, a considerable amount of energy that shows how stable these highly coordinated fullerenes are. The BE per group in the complexes (η^2-

Table 6.7 Geometric properties and fullerene-metal binding energies (BE) for (η^2-C_{60}){$Pd(PH_3)_2$}$_n$ (n = 1, 2, 4, 6) [a]

n	*Sym*	*Pd–P*	*Pd–C*	*Δ(C–C)* [b]	*P–Pd–P*	*final* θ_p [c]	*BE per group* [d]
1	C_{2v}	2.348	2.175	0.070	106.7	14.57	–0.88
2	D_{2h}	2.330	2.165	0.071	107.6	14.56	–0.82
4	D_{2h}	2.320	2.155	0.070	109.9	14.42	–0.78
6	T_h	2.320	2.181	0.063	110.2	14.17	–0.75

[a] Bond lengths in Å, angles in º and energies in eV. [b] Difference between the original bond in the free C_{60} and in the complex. [c] Pyramidalization angle (θ_p) for the carbons attached to metal unit in the complex. The θ_p for the free C_{60} is 11.67º. [d] The binding energy (BE) per group is calculated from the reaction: $C_{60} + n\{Pd(PH_3)_2\} \rightarrow (\eta^2\text{-}C_{60})\{Pd(PH_3)_2\}_n$, BE per group = ΔE/*n*; ΔE, reaction energy. BSSE = 0.05-0.06 eV.

C_{60}){$Pt(PH_3)_2$}$_n$ range from –0.96 for n = 1 to –0.81 for n = 6. The maximum number of metal groups coordinated to the C_{60} is probably imposed by the steric effects of the bulky PEt_3 ligands.

6.4.2 Pd and Ni complexes

The addition of one metal group to the C_{60} reduces only slightly the ability of the carbon cluster to accept a second metal. So, like other studies, we confirm that the interaction is highly local. However, when the number of metal groups coordinated to the fullerene increases, the BE per group decreases slightly. Indeed for Pd complexes, the BE per group ranges from –0.88 eV (n = 1, monoaddition) to –0.75 eV (n = 6, hexaaddition) (Table 6.7). For the Ni complexes the decrease was calculated to be same (Table 6.8).

The geometrical distortion caused by the polyaddition of $M(PH_3)_2$ (M = Pd, Ni) units to the C_{60} fullerene is similar to that caused by Pt units. The M–C distance increases when the number of metal units increases because the M–C bond weakens: 2.175 Å for the monoadduct (η^2-C_{60})$Pd(PH_3)_2$ and 2.181 Å when six $(PH_3)_2Pd$ units are added. The Pd double addition complex has a special stabilization, as evidenced by the Pd–C distance, which is a little shorter than the distance in the monoaddition complex. This is also observed for Pt complexes. The

Table 6.8 Geometric properties and fullerene-metal binding energies (BE) for (η^2-C_{60}){$Ni(PH_3)_2$}$_n$ (n = 1, 2, 4, 6) [a]

n	*Sym*	*Ni–P*	*Ni–C*	*Δ(C–C)* [b]	*P–Ni–P*	*final* θ_p [c]	*BE per group* [d]
1	C_{2v}	2.166	1.965	0.083	105.7	14.94	–1.73
2	D_{2h}	2.139	1.966	0.083	106.8	14.90	–1.66
4	D_{2h}	2.163	1.968	0.078	108.3	14.68	–1.63
6	T_h	2.165	1.977	0.074	107.4	14.48	–1.60

[a] Bond lengths in Å, angles in º and energies in eV. [b] Difference between the original bond in the free C_{60} and in the complex. [c] Pyramidalization angle (θ_p) for the carbons attached to metal unit in the complex. The θ_p for the free C_{60} is 11.67º. [d] The binding energy (BE) per group is calculated from the reaction: $C_{60} + n\{Ni(PH_3)_2\} \rightarrow (\eta^2\text{-}C_{60})\{Ni(PH_3)_2\}_n$, BE per group = $\Delta E/n$; ΔE, reaction energy. BSSE = 0.07-0.10 eV.

deformation in both fragments is less important in polyaddition complexes than in single- addition complexes: the P–M–P angle increases when several metals are added to the fullerene surface. For instance, the P–M–P angle is computed to be 106.7º in the (η^2-C_{60})$Pd(PH_3)_2$ complex and 110.2º in the hexaaddition complex. In the fullerene cage, the polyaddition is accompanied by the less important effect of the C–C edge pulling away from the fullerene surface. The fact that the C–C for the polyaddition complexes (0.063 Å for Pd and 0.074 Å for Ni in the (η^2-C_{60}){$M(PH_3)_2$}$_6$) increases less than the C–C bonds lengths in the monoaddition complexes (0.070 Å for Pd and 0.083 Å for Ni) confirms this idea (Tables 6.7 and 6.8).

6.4.3 Pyramidalization of carbons attached to the metal unit

The most important effect in the fullerene cage is the change in the pyramidalization angle of the carbons attached to the metal units. The degree of pullout may be indicated by the increase in the pyramidalization angle. The pyramidalization angle for free C_{60} is equal to 11.67º for all atoms and increases in all C–C bonds coordinated to a metal unit. Metal attachment causes an increase in the pyramidalization angle in the local interaction area because it pulls the C–C bond away from the edge. When metals are added successively to the fullerene cage the BE and

pyramidalization angle decrease slightly. The higher the pyramidalization angle produced by these metal additions in the coordinated C–C, the more stable the complex obtained will be. The pyramidalization angle, and therefore the distortion, is higher in the monoaddition complexes than in the rest. In this respect, Figure 6.5 shows a clear positive correlation between the BE per added group and the pyramidalization angle for all series of polyaddition exohedral metallofullerenes. It should be pointed out that although the decrease in the BE is very small, the change in the pyramidalization angle is sensitive. For instance, pyramidalization angles ranges between 15.47º and 14.88º for the series (η^2-C_{60}){$Pt(PH_3)_2$}$_n$ n = 1, 2, 4, 6. Ni and Pd complexes follow the same trend: that is to say, the pyramidalization angle in the hexaaddition complexes (14.17º for Pd and 14.48º for Ni) is lower than in the monoaddition complexes (14.57º and 14.94º, respectively). After the metal additions, the most pyramidalised carbons are those attached to the metal units. All these features can be attributed to decrease in the π* orbital energy of the coordinated C–C bond which, in turn, leads to an increase in the π back-donation from the *d* metal orbitals to the fullerene.

6.5 MONOADDITION COMPLEXES OF C_{70} AND C_{84}

Our analysis of the (η^2-C_{70})$Pt(PH_3)_2$ and (η^2-C_{84})$Pt(PH_3)_2$ complexes showed us how to evaluate the effect that the fullerene curvature and the different types of the C–C bonds have on the strength of the bond between the metal unit and the fullerene cage. The C_{70} and C_{84} are less spherical than C_{60} and their cages have carbons with different pyramidalization angles. The curvature of these higher fullerenes is different on each part of the fullerene surface.

6.5.1 C_{70}

Table 6.9 Geometric properties and binding energies (BE) for (η^2-C_{70})Pt(PH$_3$)$_2$ and (η^2-C_{84})Pt(PH$_3$)$_2$ [a]

Cage	*C–C bond* [b]	*Sym.*	*Pt–C*	*Δ(C–C)* [c]	*initial* θ_p [d]	*final* θ_p [d]	*BE* [e]	*BSSE* [f]
C_{70}	Ca–Cb	C_s	2.140	0.104	11.92	15.66	–1.04	0.05
	Cc–Cc	C_s	2.142	0.097	11.49	15.25	–0.95	0.05
	Ce–Ce*	C_{2v}	2.183	0.115	8.60	12.69	–0.22	0.05
D_{2d}-C_{84}:***23***	C42–C43	C_{2v}	2.175	0.088	10.80	14.35	–1.00	0.11
	C9–C10	C_2	2.152	0.079	10.68	14.34	–0.91	0.08
	C5–C6	C_s	2.163	0.076	10.98	14.53	–0.83	0.08
	C2–C3*	C_s	2.165	0.098	7.67	11.94	–0.33	0.08
D_2-C_{84}:***22***	C9–C10	C_1	2.164	0.082	10.73	14.26	–0.94	0.09
	C32–C53	C_2	2.148	0.082	10.71	14.48	–0.82	0.08
	C7–C22	C_1	2.153	0.079	10.91	14.64	–0.80	0.08

[a] Bond lengths in Å, angles in º and energies in eV. [b] All are pyracylene C–C bond types except those marked with * which are pyrene types (Figure 6.1 for C_{70} and Figure 6.2 and 6.3 for C_{84}). [c] Difference between the bond distance in the free fullerene and in the complex. For the free D_{5h}-C_{70}, Ca–Cb: 1.398 Å, Cc–Cc: 1.392 Å and Ce–Ce: 1.469 Å; for D_{2d}-C_{84}:**23**, C42–C43: 1.375 Å, C9–C10: 1.369 Å, C5–C6: 1.377 Å and C2–C3: 1.461 Å; for the D_2-C_{84}:**22**, C9–C10: 1.373 Å, C32–C53: 1.369 Å and C7–C22: 1.377. [d] Pyramidalization angle for the coordinated carbon bond in the free fullerene (initial θ_p) and in the complex (final θ_p). [e] Binding energy (BE). [f] Basis set superposition error (BSSE)

The C_{70} is more curved at the poles and flatter at the equator. The Ce carbons at the equator of the molecule are the least pyramidalised with θ_p = 8.60º, whereas the Ca and Cb carbons at the poles have the highest pyramidalization angle, 11.92º. The pyramidalization angle of the other carbons is between these values. To determine the dependence of the fullerene-metal BE on the fullerene curvature, we studied the coordination of the Pt(PH$_3$)$_2$ unit to the Ce–Ce, Cc–Cc and Ca–Cb bonds (Figure 6.1 and Appendix A.4). Like in C_{60}, the computed and experimental[39] geometries for the free C_{70} are in excellent agreement. The computed bond lengths of the pyracylene Cc–Cc and Ca–Cb bonds, 1.392 Å and 1.398 Å (Table 6.9),

respectively, are similar to those of the 6:6 C–C bonds in C_{60}. The Ce–Ce bond lengths of 1.469 Å corresponds to a 6:6 ring junction abutted by two hexagons, corresponding to a pyrene type. According to a Hückel analysis the π-bond order follows the same trend as pyramidalization angle. The highest π-bond orders are in the poles, Ca–Cb and Cc–Cc bonds, while the equator is more aromatic with low π-bond order in the Ce–Ce bond.[40]

When a $Pt(PH_3)_2$ unit is linked to the Ca–Cb bond, the deformation of the fullerene cage and the geometry of the $Pt(PH_3)_2$ unit is similar to that observed in the C_{60} derivative (compare Tables 6.3 and 6.9). So, in the optimised organometallic complexes the C–C bonds are lengthened and pulled away from the fullerene surface increasing the pyramidalization angle between 3-4º. The structure of this complex is given in Figure 6.4b. In consonance with this similarity in the geometries, both complexes differ in the BE to give the fullerene cage and the metal unit in only 0.08 eV more favorable to C_{70} addition. When a metal unit coordinates the fullerene through the Cc–Cc bond, the complex is somewhat less stable and the BE is –0.95 eV, 0.09 eV lower than for the most stable isomer. The DE for the complex in which the metal unit is linked to the carbons at the equator is only 0.22 eV. This lower energy is because of the different nature of the 6:6 Ce–Ce bonds (pyrene type) and the smaller pyramidalization angle of the Ce carbons. Note that this later energy is even smaller than that found for the C_{60} derivative with the metal unit coordinated to the 6:5 C–C bond. On the other hand, the relatively short Pt–C bond lengths, 2.183 Å, do not reveal the significant instability of the isomer with the metal unit bound to a Ce–Ce bond.

6.5.2 C_{84}

Balch and co-workers demonstrated that the addition of $Ir(CO)Cl(PPh_3)_2$ to a benzene solution of a mixture of C_{84} isomers yielded the $(\eta^2\text{-}C_{84})Ir(CO)Cl(PPh_3)_2$ complex. The X-ray analysis of this system showed that the fullerene cage corresponds to the D_{2d}-C_{84}:**23** isomer. However, the separation of C_{84} isomers that was achieved through crystallization of the $(\eta^2\text{-}C_{84})Ir(CO)Cl(PPh_3)_2{\cdot}4C_6H_6$ adduct was not complete. Examination of the residual electron density within the fullerene portion of the adduct indicated that another isomer of C_{84} was probably

present. It could be the most stable and experimentally found D_2-C_{84}:**22** isomer. At this level of computation, D_2-C_{84}:**22** isomer is slightly more stable than D_{2d}-C_{84}:**23** isomer by 0.05 eV. According to the Taylor numeration, the coordination of the iridium atom takes place at the C42–C43 bond,[41] one of the three distinct pyracylene C–C bond types of the D_{2d}-C_{84}:**23** isomer (C5–C6, C9–C10 and C42–C43, Figure 6.2). These three bonds have the shortest C–C distances (~ 1.37 Å) and the highest pyramidalised carbons of all 6:6 C–C bonds ($\theta_p \approx 11.0^o$). Moreover, according to Hückel calculations the pyracylene C–C bonds have the highest π-bond order. So, in accordance with these criteria, the pyracylene types should be the most reactive. On the other hand, the pyrene C–C bond types contain the longest 6:6 C–C bonds (~ 1.46 Å) and the corresponding carbons have small pyramidalization angles (~ 8º). Appendix A.8 describes the 19 distinct C–C bonds for the D_{2d}-C_{84}:**23** isomer. These geometrical parameters suggest that pyrene types should be the least reactive of the 6:6 C–C bonds. To evaluate the strength of the fullerene-metal bond we studied the coordination of the Pt(PH$_3$)$_2$ unit to the three pyracylene 6:6 C–C bond types and to the C2–C3 bond, one of the three pyrene 6:6 C–C bond types. The addition to the latter will allow us to establish an energy range for the 6:6 C–C bonds. The BE values in Table 6.9 fully confirm that the most reactive site corresponds to the C42–C43, the coordination position observed by Balch in the (η^2-C_{84})Ir(CO)Cl(PPh$_3$)$_2$ Vaska-type complex. The BE of –1.00 eV is only somewhat lower than that found at the same level of computation for the C_{60} and for the most reactive site in the C_{70}. The structure of the organometallic complex linked to the C42–C43 bond is given in Figure 6.4c. The BE for the other two pyracylene C–C bond types (C9–C10 and C5–C6) are –0.91 and –0.83 eV, respectively. Clearly, the pyrene C–C bond types are much less reactive since the BE associated to the coordination of a Pt(PH$_3$)$_2$ unit to C2–C3 is only –0.33 eV, a value similar to that determined for the 6:5 C–C bond in C_{60}. Also, the BSSE was calculated for exohedral complexes of C_{70} and C_{84}, giving a small range of values between 0.05 and 0.11 eV. The most reactive sites according to Hückel calculations, bond lengths and pyramidalization angles of the D_2-C_{84}:**22** isomer were tested. These correspond to the three pyracylene 6:6 C–C bond types: C9–C10, C32–C53 and C7–C22. See Appendix A.7 for a

Table 6.10 Mulliken net charges for several $Pt(PH_3)_2$ exohedral metallofullerenes

Fullerene cage	*C–C bond* [a]	*Metal Number*	*C_2* [b]	*Pt*	$Pt(PH_3)_2$ Mulliken [c]
C_{60}	6:5	1	–0.632	0.292	0.614
	6:6	1	–0.656	0.330	0.688
	6:6 [d]	2	–0.688	0.327	0.649
	6:6 [d]	4	–0.676	0.294	0.559
	6:6 [d]	6	–0.670	0.281	0.512
C_{70}	Ca–Cb	1	–0.676	0.326	0.698
	Cc–Cc	1	–0.646	0.336	0.689
	Ce–Ce	1	–0.662	0.243	0.561
*D_{2d}-C_{84}:**23***	C42–C43	1	–0.589	0.312	0.664
	C9–C10	1	–0.604	0.330	0.659
	C5–C6	1	–0.590	0.265	0.627
	C2–C3	1	–0.730	0.257	0.576
*D_2-C_{84}:**22***	C9–C10	1	–0.595	0.300	0.660
	C32–C53	1	–0.612	0.328	0.661
	C7–C22	1	–0.614	0.288	0.658

[a] C–C bond linked to the metal (see Figure 6.1 and Appendix A.4 for C_{70} and Figure 6.2, Figure 6.3, Appendix A.7 and A.8 for C_{84}). [b] Net charge for the C_2 unit coordinated to the metal. [c] Mulliken net charges for the whole $Pt(PH_3)_2$ unit. [d] Average values.

complete description of all types of C–C bonds of the *D_2*-C_{84}:**22** isomer. Any of them lead to a more stable isomer than the addition of the $Pt(PH_3)_2$ unit to the C42–C43 bond in the *D_{2d}*-C_{84}:**23** (Table 6.9). But these calculations do not prevent the formation of organometallic complexes from the *D_2*-C_{84}:**22** isomer. In fact, experimentally the most stable adduct from the *D_2*-C_{84}:**22** could be found together with the most stable adduct from the *D_{2d}*-C_{84}:**23** isomer. It is interesting to remark that although the free *D_2*-C_{84}:**22** isomer is the most stable isomer overall, the isomer present in the most stable (η^2-C_{84})$Pt(PH_3)_2$ complex isomer comes from the *D_{2d}*-C_{84}:**23**

isomer. The reason of this is because the C42–C43 bond of the D_{2d}-C_{84}:**23** provide a better reactive site than the lower reactive C9–C10 of the D_2-C_{84}:**22** according to pyramidalization angle and MBO. To sum up, all data concordance with the prevalent presence of the D_{2d}-C_{84}:**23** isomer as adduct and the relation 2:1 favorable to the D_2-C_{84}:**22** isomer in the mixture of free isomers.

6.5.3 Electron charge transfer

The Dewar-Chatt-Ducanson model is appropriate for describing the (η^2-C_2)-M bond. Previous calculations illustrate that the π back-donation dominates over the σ donation in these complexes and, therefore, there is an electron charge transfer from the metal unit to the fullerene cage. According to the Mulliken charges, each $Pt(PH_3)_2$ unit coordinated to the fullerene surface transfers approximately 0.6 electron, which are practically at the carbons linked to the metal unit (Table 6.10). The electron charge transfer is similar in the three fullerene cages studied with the characteristic that the complexes with the strongest fullerene-metal bond have the highest electron charge transfers. For instance, in the series of (η^2-C_{60})$\{Pt(PH_3)_2\}_n$ (n = 1, 2, 4, 6) 0.688 *e* are transferred from the $Pt(PH_3)_2$ unit to C_{60} in the monoaddition complex while 0.512 *e* are transferred per unit in the hexaaddition complex. Notice from values of Table 6.10 that the BE between the metal unit and C_{60} appears to be strongly correlated with the amount of electron charge transferred to the carbon cluster.

6.6 PREDICTION OF THE MOST REACTIVE SITES

The bonding scheme between the $M(PH_3)_2$ units and the fullerene cages is of coordinative type. It is based on the σ donation of π-electrons from the ligand to the metal atom and on the formation of a π-bond by back-donation from the metal *d*-orbitals to the π* C–C bond orbitals. All the factors that affect the strength of the coordinated C–C bond will modify the BE between both fragments. To increase the σ donation, an electron-rich C–C double bond is required, or in other words with a high π-bond order or MBO. Alternatively, the C–C bond lengths —which are completely correlated to the MBO— can also be indicative of the strength of the

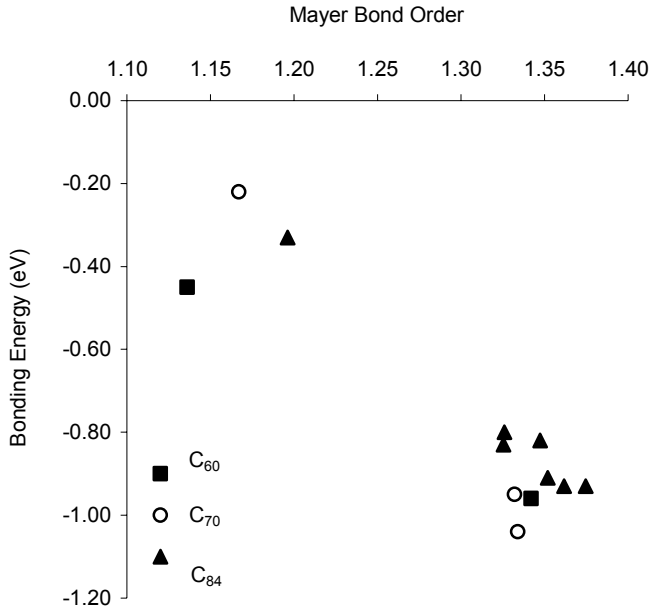

Figure 6.6 Mayer bond order (MBO) versus fullerene-metal binding energies (BE) for the C_{60}, C_{70} and C_{84} complexes

hypothetical fullerene-metal bond. Moreover, the pyramidalization angle of the free carbons can be used to estimate *a priori* this strength: the most pyramidalised carbons of the free fullerene (initial θ_p) have more sp^3 character than the less pyramidalised ones and, consequently, the interaction between them and the metal unit is more effective as some recent studies have shown.[42] This geometric parameter, then, can be used to predict the most reactive sites on the fullerene because it shows that the most pyramidalised carbons will be the most favourable sites for metal additions. In resume, the final pyramidalization angle (final θ_p) is indicative of how strong the bond is between both fragments, but the initial pyramidalization angle is also a reliable indicative parameter for this measure. Both characteristics (high pyramidalization angle and high MBO) do not always occur simultaneously because a high pyramidalization angle of the carbons is often accompanied by a long C–C bond length. Hence, the order of the BE can be estimated by taking into account only the pyramidalization angle and the MBO of the C–C bond which will react in the free fullerene. In the

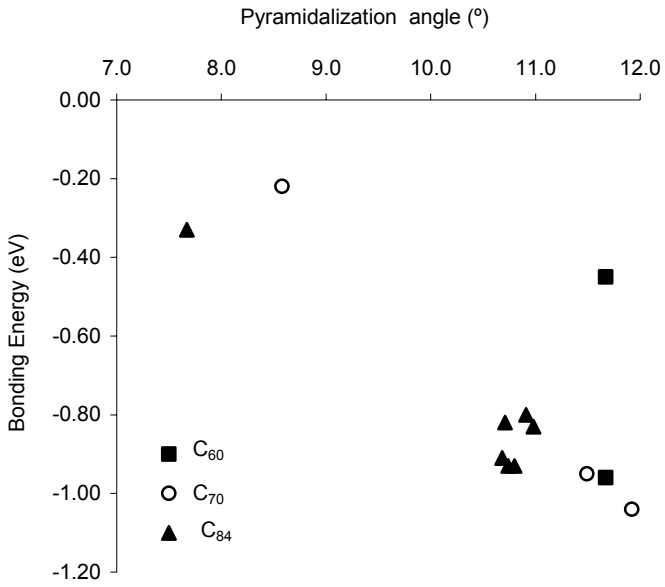

Figure 6.7 Pyramidalization angle (θ_p) versus fullerene-metal binding energies (BE) for the C_{60}, C_{70} and C_{84} complexes

most difficult cases, when both parameters are not conclusive, the final reactivity prediction will be a compromise between both parameters.

The types of all the C–C bonds, the bond lengths, the pyramidalization angles and the MBOs for all the different C–C bonds of the C_{60}, C_{70}, D_{2d}-C_{84}.**23** and D_2-C_{84}:**22** free fullerenes are given in Appendix A.2, A.4, A.8 and A.7, respectively. For a graphical representation of the different C–C bond types in the IPR fullerenes (Appendix A.1). A first inspection reveals that high MBOs and highly pyramidalised carbons are found in the pyracylene 6:6 C–C bond types (***A*** type). Hence, this C–C bond type will always tend to form the most stable complexes through metal addition reactions. On the other hand, pyrene 6:6 C–C bond types (***C*** type) show opposite features. The corannulene 6:5 C–C bond types (***D*** type) and the 6:6 C–C bonds abutted by a hexagon and a pentagon (***B*** type) have intermediate values. We correlated the BE versus the MBO in Figure 6.6, versus the pyramidalization angle in Figure 6.7 and versus the bond lengths in Figure 6.8 of the various free C–C bonds for the monoaddition complexes

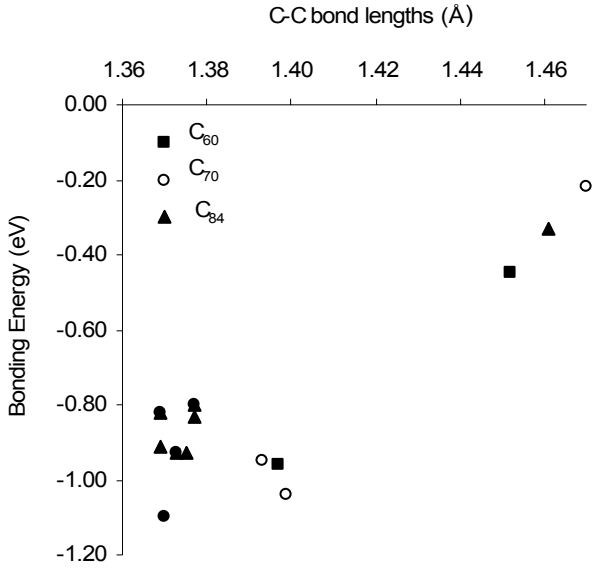

Figure 6.8 Free C–C bond distance versus fullerene-metal binding energies (BE) for the C_{60}, C_{70} and C_{84} complexes

of the C_{60}, C_{70}, D_{2d}-C_{84}:**23** and D_2-C_{84}:**22** free fullerenes. The trend is clear in Figure 6.6 and 6.7 except for the $Pt(PH_3)_2$ addition to the 6:5 C–C bond of C_{60} (square dot).

High MBOs and high initial pyramidalization angles are accompanied by more stable organometallic complexes and are a completely conclusive measure for predicting the stability of a metal unit addition to a C–C bond in a fullerene. It is important to point out that the D_{2d}-C_{84}:**23** isomer has the strongest C–C bond in the group of fullerenes above mentioned: the C42–C43 bond with an MBO of 1.375. Consequently, it seems that this isomer should be the most reactive toward addition reactions. However, it does not have the highest BE. It is found in the metal addition reaction to the Ca–Cb in C_{70}. This other C–C bond has a lower MBO, 1.334, but a much higher pyramidalization angle of 11.92° than the first one, 10.80°. Finally, we should mention that simple inspection of the bond lengths is also a good indicative parameter of the strength of the future fullerene-metal bond (Figure 6.8).

6.7 CONCLUDING REMARKS

DFT calculations were performed on the series of complexes: (η^2-C_{60}){$M(PH_3)_2$}$_n$ (M = Pt, Pd, Ni; n = 1, 2, 4, 6), (η^2-C_{70})$Pt(PH_3)_2$ and (η^2-C_{84})$Pt(PH_3)_2$ so that we could analyze how important the effect of the fullerene curvature on the BE was when mono- and polyaddition of metal units occurs. Pyracylene 6:6 C–C bonds are the most reactive sites in all the cages analyzed: C_{60}, C_{70} and C_{84}. The binding energy (BE) between the $Pt(PH_3)_2$ unit and the fullerene is almost independent of the size of the cage and of the number of coordinated metals on the fullerene surface. Contrarily, the curvature and C–C bond type determine the strength of the coordination bond. Relatively large basis sets must be used if energies are to be consistent. Finally, we investigated the correlation of the characteristics of the reactive C–C bonds of the free fullerenes with their BEs in order to obtain parameters for predicting the stability of these exohedral metallofullerenes. The main conclusions are:

Coordination bond. The $M(PH_3)_2$ metal unit is, in all cases, η^2 coordinated to a pyracylene 6:6 C–C bond type. Various possibilities of coordination on the fullerene surface have been analyzed but the η^2 coordination is always the most stable overall, indicating that the fullerene has an alkene character and not a benzenoid aromatic character. More precisely, the fullerene in these exohedral metallofullerenes acts like an electron-deficient alkene such as $C_2(CN)_4$ rather than a simple C_2H_4.

Electronic structure. The most widely accepted model for the patterns of the (η^2-C_2)-M bond is the one proposed by Dewar, Chatt and Duncanson. It involves forming a σ-donation bond from π ligand orbitals to the *d* metal orbitals and a π-back-donation bond from *d* metal orbitals to the π* C–C orbital. In these complexes, the π back-donation dominates over the σ-donation.

Monoaddition complexes of C_{60}. The metal unit is always coordinated to a 6:6 C–C bond because the coordination to a 6:5 C–C bond is very unfavorable: the BE between the fullerene and the metal unit is –0.96 eV for 6:6 coordination in contrast to –0.45 eV for 6:5 coordination.

The metal attachment lengthens the C–C bond and a pulls away the C–C edge from the fullerene surface reflected by the increment of the pyramidalization angle (θ_p). At the best level of calculation (TZP basis set for all atoms), the energy involved in the coordination of a $Pt(PH_3)_2$ unit to a C_{60} is almost the same as, or a little higher than the energy involved in the coordination of an ethylene. Also, the BE is well reproduced if the fullerene cage is described by a mixed basis set: TZP for the carbons belonging to the coordinated pyracylene and DZP for the others. The BE increases in the order Pd ≈ Pt < Ni. The basis set superposition error (BSSE) is calculated to be very small (0.05-0.10 eV) at the best level of computation, so it can be neglected. To sum up, the experimental geometries were well reproduced but in general it still appears a discrepancy between the experimental and calculated BEs for these organometallic complexes of fullerenes and ethylene.

Polyaddition complexes of C_{60}. When the number of metals attached to the fullerene cage increases, the BE decreases only slightly, which emphasizes the local nature of the fullerene-metal interaction. Also a less geometrical distortion is observed in the fragments when the polyaddition occurs: the P–M–P angle and the M–C bond lengths increase slightly. But the most important effect is the decrease in the pyramidalization angle of the coordinated C–C bond, which correlates well with the decrease in the BE per group. Recently, Melchor and coworkers showed that the curvature is a prerequisite of atomic phosphorous for bonding to polycyclic hydrocarbons and curved graphite surfaces.[43]

Monoaddition complexes of C_{70} and C_{84}. In the C_{70}, the most reactive site is that of the C–C bond with the most pyramidalised carbons in the free fullerene: the pyracylene 6:6 Ca–Cb bond. For C_{84}, two different isomers have been found experimentally (isomer **22** and **23**) but principally only the D_{2d}-C_{84}:**23** isomer formed the exohedral compound. Our calculations confirm that the most reactive site of the D_{2d}-C_{84}:**23** isomer, the pyracylene 6:6 C42–C43 bond , is a more reactive by 0.06 eV than the most reactive site of the D_2-C_{84}:**22** isomer, C9–C10 bond. It is noteworthy that the DE of the most stable monoaddition complexes of C_{70} and C_{84} is similar to that of the (η^2-C_{60})$Pt(PH_3)_2$, but the reactivity of the distinct 6:6 C–C bonds can be

quite different. Hence, for example, the addition to a pyracylene C–C bond type in C_{84} can be more favorable than to a pyrene C–C bond type by 0.67 eV, almost the same energy difference found between the most and the least reactive site in C_{70}.

Prediction parameters. We also explored the role that the pyramidalization angle of carbons plays in the nature of fullerene-metal interactions. The strain within these curved clusters and the strain release that accompanies adduct formation are important factors which will determine the strength of the fullerene-metal interaction. As was expected, the initial values of bond lengths, the pyramidalization angles and MBOs of the free C–C bonds can give us conclusive proofs on the future strength of the bond between the C–C bond and the metal unit. The correlation between these parameters and the BE for C_{60}, C_{70} and C_{84} fullerenes has been plotted to corroborate the idea.

REFERENCES AND NOTES

[1] (a) Hawkins, J. M.; Meyer, A.; Lewis, T. A.; Loren, S.; Hollander, F. J. *Science* **1991**, *252* 312. (b) Hawkins, J. M. *Acc. Chem. Res.* **1992**, *25*, 150. (c) Stephens, A. H. H.; Green, M. L. H. *Adv. Inorg. Chem*. **1997**, *44*, 1.

[2] (a) Balch, A. L.; Olmstead, M. M. *Chem. Rev.* **1998**, *98*, 2123. (b) Balch, A. L. *In the Chemistry of Fullerenes*; Taylor, R., Ed.; *Advanced Series in Fullerenes*; World Scientific Publishing Co.; Singapore, 1995; Vol. 4, p 220.

[3] Fagan, P. J.; Calabrese, J. C.; Malone, B. *Science* **1991**, *252*, 1160.

[4] (a) Lerke, S. A.; Parkinson, B. A.; Evans, D. H.; Fagan, P. J. *J. Am. Chem. Soc.* **1992**, *114*, 7807. (b) Bashilov, V. V.; Petrovskii, P. V.; Sokolov, V. I.; Lindeman, S. V.; Guzey, I. A.; Struchkov, Y. T. *Organometallics* **1993**, *12*, 991.

[5] (a) Fagan P. J.; Calabrese, J. C.; Malone, B. *J. Am. Chem. Soc.* **1991**, *113*, 9408. (b) Fagan, P. J.; Calabrese, J. C.; Malone, B. *Acc. Chem. Res.* **1992**, *25*, 134.

[6] (a) Balch, A. L.; Catalano, V. J.; Lee, J. W. *Inorg. Chem.* **1991**, *30*, 3980. (b) Vértes, A.; Gál, M.; Wagner, F. E.; Tuczek, F.; Gütlich, P. *Inorg. Chem.* **1993**, *32*, 4478.

[7] Balch, A. L.; Catalano, V. J.; Lee, J. W.; Olmstead, M. M.; Parkin, S. R. *J. Am. Chem. Soc.* **1991**, *113*, 8953.

[8] Balch, A. L.; Ginwalla, A. S.; Noll, B. C.; Olmstead, M. M. *J. Am. Chem. Soc.* **1994**, *116*, 2227.

[9] Balch, A. L. ; Lee, J. W.; Noll, B. C. ; Olmstead, M. M. *J. Am. Chem. Soc.* **1992**, *114*, 10984.
[10] Balch, A. L.; Lee, J. W.; Noll, B. C.; Olmstead, M. M. *Inorg. Chem.* **1994**, *33*, 5238.
[11] Balch, A. L.; Lee, J. W.; Olmstead, M. M. *Angew. Chem., Int. Ed. Engl.* **1992**, *31*, 1356.
[12] López, J. A.; Mealli, C. *J. Organomet. Chem.* **1994**, *478*, 161.
[13] Fowler, P. W.; Manoloupoulus, D. E. *An Atlas of Fullerens*, Oxford University Press, Oxford, **1995**.
[14] Balch, A. L.; Hao, L.; Olmstead, M. M. *Angew. Chem., Int. Ed. Engl.* **1996**, *35*, 188.
[15] (a) Zhang, B. L.; Wang, C. Z.; Ho, K. M. *J. Chem. Phys.* **1992**, *96*, 7183. (b) Wang, X. Q.; Wang, C. Z.; Zhang, B. L.; Ho, K. M. *Phys. Rev. Lett.* **1992**, *69*, 69. (c) Wang, X. Q.; Wang, C. Z.; Zhang, B. L.; Ho, K. M. *Chem. Phys. Lett.* **1993**, *207*, 349.
[16] Stone, A. J.; Wales, D. *J. Chem. Phys. Lett*. **1986**, *128*, 501.
[17] (a) Kikuchi, K.; Nakahara, N.; Wakabayashi,T.; Suzuki, S.; Shiromaru, H.; Miyake, Y.; Saito, K.; Ikemoto, I.; Kainosho, M.; Achiba, Y. *Nature* **1992**, *357*,142. (b) Manolopoulos, D. E.; Fowler, P. W.; Taylor, R.; Kroto, H. W.; Walton, D. R. M. *J. Chem. Soc., Faraday Trans.* **1992**, *88*, 3117.
[18] Koga, N; Morokuma, K. *Chem. Phys. Lett.* **1993**, *202*, 330.
[19] Bo, C.; Costas, M.; Poblet, J. M. *J. Phys. Chem*. **1995**, *99*, 5914.
[20] Nunzi, F.; Sgamellotti, A.; Re, N.; Floriani, C.; *Organometallics* **2000**, *19*, 1628.
[21] Nunzi, F.; Sgamellotti, A.; Re, N.; *J. Chem. Soc., Dalton Trans*. **2002**, 399.
[22] Dedieu, A. *Chem. Rev.* **2000**, *100*, 543.
[23] (a) Lichtenberger, D. L.; Wright, L. L.; Gruhn, N. E. Rempe, M. E. *Synth. Met.* **1993**, *59*, 353. (b) Lichtenberger, D. L.; Wright, L. L.; Gruhn, N. E. Rempe, M. E. *J. Organomet. Chem.* **1994**, *478*, 213.
[24] Jemmis, E. D.; Maniharan, M.; Sharma, P. K. *Organometallics* **2000**, *19*, 1879-1887
[25] (a) Dewar, M. J. S. *Bull. Soc. Chim. (Fr.)* **1951**, *18*, C71. (b) Chatt., J.; Duncanson, L. A. *J. Chem. Soc.* **1953**, 2939.
[26] Haddon, R. C. *Science* **1993**, *261*, 1545.
[27] (a) Haddon, R. C.; Scott, L. T. *Pure Appl. Chem.* **1986**, *58*, 137. (b) Haddon, R. C. *J. Am. Chem. Soc.* **1986**, *108*, 2837. (c) Haddon, R. C.; Chow, S. Y. *J. Am. Chem. Soc.* **1998**, *120*, 10494.
[28] (a) Yang, S. H.; Pettiette, C. L.; Concienciao, J.; Cheshnowsky, O. ; Smalley, R.E. *Chem. Phys. Lett.* **1991**, *139*, 233. (b) Lerke, S. A.; Parkinson, B. A.; Evans, D. H.; Fagan, P. J. *J. Am. Chem. Soc.* **1992**, *114*, 7807.

[29] Stephens, A. H. H.; Green, M. L. H. *Adv. Inorg. Chem.* **1997**, *44*, 1.
[30] In Chapter 5 this complex is written as $C_{58}Pt(C_2H_4)$. In Chapter 6 we use the order: ligand + metal unit, which is the order in the $(\eta^2\text{-}C_{60})Pt(PH_3)_2$ complexes. So the chemical name $C_{58}Pt(C_2H_4)$ becomes $(\eta^2\text{-}C_2H_4)C_{58}Pt$.
[31] (a) Ziegler, T.; Rauk, A. *Teor. Chim. Acta* **1977**, *46*, 1. (b) Ziegler, T.; Rauk, A. *Inorg. Chem.* **1979**, *18*, 1558.
[32] (a) Morokuma, K. *J. Chem. Phys.* **1971**, *55*, 1236. (b) Kitaura, K.; Morokuma, K. *Int. J. Quantum. Chem.* **1976**, *10*, 325.
[33] Morokuma, K.; Borden. W. T. *J. Am. Chem. Soc.* **1991**, *113*, 1912.
[34] Ziegler, T. Tschinke, V.; Baerends, E. J.; Snijiders, J. G.; Ravenek, W. *J. Phys. Chem.* **1989**, *93*, 3050.
[35] Frenking, G; Antes, I.; Böhme, M.; Dapprich, S.; Ehlers, A. W.; Jonas, V.; Neuhaus, A.; Otto, M.; Stegmann, R. Veldkamp, A.; Vyboishchikov, S. F. *In Reviews in Computational Chemistry*; Lipkowitz, K. B. Boyd, D. B. Eds.; VCH Publishers: New York, **1996**; Vol. 8, p63.
[36] (a) Mortimer, C. T. *Rev. Inorg. Chem.* **1984**, *6*,233. (b) Martinho-Simoes, J. A.; Beauchamp, J. L. *Chem. Rev.* **1990**, 629 and references therein.
[37] Rosa, A.; Ehlers, A. W.; Baerends, E. J.; Snidjers, J. G.; te Velde, G. *J. Phys. Chem*. **1996**, *100*, 5690.
[38] Nunzi, F.; Sgamellotti, A.; Re, N.; Floriani, C. *J. Chem. Soc., Dalton Trans.* **1999**, 3487.
[39] Hedberg, K.; Hedberg, L.; Bühl, M.; Bethune, D.S.; Brown, C. A.; Dorn, H. C.; Johnson. R. D. *J. Am. Chem. Soc.* **1997**, *119*, 5314.
[40] Taylor, R. *J. Chem. Soc., Perkin Trans. 2* **1993**, 813.
[41] Notice that Ir links to C32–C53 bond in reference but this C–C bond is equivalent also to C42–C43 bond according to numbering scheme proposed by Taylor for D_{2d}-C_{84}:**23** in reference 40.
[42] Park, S.; Srivastava, D.; Cho; K. *Nanotechnology* **2001**, *12*, 245.
[43] Melchor, S.; Dobado, J. A.; Larsson, J. A.; Greer, J. C. *J. Am. Chem. Soc.* **2003**, *125*, 2301.